

Labelless AC Impedimetric Antibody Based Sensors with pg ml^{-1} Sensitivities for Point-Of-Care Biomedical Applications.

Andrew C. Barton¹, Goulielmos-Zois Garifallou¹, Frank Davis¹, Stuart D. Collyer², Georgios Tsekenis¹, Paul A. Millner³, Tim D. Gibson⁴ and Séamus P. J. Higson^{*1}.

¹Cranfield Health, Cranfield University, Silsoe, Beds, MK45 4DT, UK.

²Microarray Ltd, PO Box 88, Manchester, M60 1QD, UK.

³School of Biochemistry and Molecular Biology, University of Leeds, Leeds, LS2 9JT, UK.

⁴T and D Technology Ltd, Wakefield, W. Yorks, WF3 4AA, UK.

*Corresponding author. Fax (+44) 01525 863433, email s.p.j.higson@cranfield.ac.uk

Abstract.

This paper describes the development and characterisation of labelless immunosensors for (a) the cardiac drug digoxin and (b) bovine serum albumin (BSA). Commercial screen-printed carbon electrodes were used as the basis for the sensors. Two methods were used to immobilise antibodies at the electrode surface. Aniline was electropolymerised onto these electrodes to form a thin planar film of conductive polyaniline; the polyaniline film was then utilised as a substrate to immobilise biotinylated anti-digoxin using a classical avidin-biotin affinity approach. As an alternative approach, poly(1,2-diaminobenzene) was electrodeposited onto the carbon electrodes - and this modified surface was then sonochemically ablated to form an array of micropores. A second electropolymerisation step was then used to co-deposit

conductive polyaniline along with antibodies for BSA within these pores to produce a microarray of polyaniline protrusions with diameters of several μm containing entrapped anti-BSA.

The resulting antibody grafted electrodes were interrogated using an AC impedance protocol before and following exposure to digoxin or BSA solutions, along with control samples containing a non-specific IgG antibody. The impedance characteristics of both types of electrode were changed by increasing concentrations of antigen up to a saturation level. Calibration curves were obtained by subtraction of the non-specific response from the specific response, thereby eliminating the effects of non-specific adsorption of antigen. Both the use of microelectrode arrays and affinity binding protocols showed large enhancements in sensitivity over planar electrodes containing entrapped antibodies and gave similar sensitivities to our other published work using affinity based planar electrodes. Detection limits were of the order of 0.1 ng ml^{-1} for digoxin and 1.5 ng ml^{-1} for BSA.

Keywords. ac impedance, immunosensor, polyaniline, microelectrode, BSA, digoxin.

1. Introduction

The principle of immunoassays was first established in 1959 (Yalow and Berson 1959) and their work led to the development of the widely used radioimmunoassay to determine insulin-binding antibodies in human serum, using samples obtained from subjects that had been treated with insulin. Later, within unconnected work (Clark and Lyons 1962), the concept of a biosensor was pioneered. These workers exploited the selectivity of enzymes for analytical purposes via a methodology which involved immobilising enzymes on the surface of electrochemical sensors and measuring the oxygen consumption by the glucose oxidase enzymatically catalysed oxidation of glucose. This basic idea has remained virtually unchanged since the original design, although the field has undergone continual technological developments over the last forty years.

The incorporation of antibodies into conducting polymer films was first reported (John *et al* 1991) in 1991. Pyrrole was galvanostatically polymerised onto a platinum wire substrate from a solution which contained anti-human serum albumin (anti-HSA). The antibody was incorporated into the polypyrrole film and the pyrrole anti-HSA electrode found to give a specific electrochemical response to HSA. Since this early work there has been burgeoning interest in the development of electrochemical immunosensors - as detailed in several recent reviews (Rodriguez-Moraz *et al* 2006, Diaz-Gonzales *et al* 2005, Cosmier 2005).

Antibody-antigen interactions are by their very nature complex and it is thought necessary that the affinity reaction be minimally perturbed by the fabrication procedure to give reproducible response characteristics. We have previously shown that up to 2-3 μg antibodies for BSA and digoxin may be successfully incorporated

into conducting polymer films by entrapment in a growing polypyrrole film with no detrimental effect to antibody activity (Grant *et al* 2003). Electrochemical interrogation of these films demonstrated selective interactions with the target antigens. Further work utilised an AC impedance protocol (Grant *et al* 2005) as the method of interrogation for these films - and led to the development of immunosensors for digoxin and bovine serum albumin. Later work by our group utilised polyaniline coated screen-printed planar carbon electrodes as substrates for immobilisation of antibodies utilising the classical avidin-biotin interaction. This enabled the construction of immunosensors for the fluoroquinolone antibody ciprofloxacin (Garifallou *et al* 2007) and myelin basic protein - a marker for conditions such as stroke and multiple sclerosis (Tsekenis *et al* 2008).

Our group has also pioneered the development of sonochemically fabricated microarrays of conductive polymers (Higson 1996), the schematic for the formation of which is shown within figure 1. Poly(1,2-diaminobenzene) can be electrodeposited on a variety of conductive surfaces to form an insulating layer¹⁵. We have utilised commercial screen printed 3 electrode strips as the basis for these sensors. The working electrodes are initially coated with a thin film (50-70 nm thickness) of an insulating polymer formed by the electrochemical deposition of 1,2-diaminobenzene (Myler *et al* 1997). An advantage of this process is that it is self-limiting, making it highly reproducible. Sonochemical ablation is then used to ablate or “drill” holes in this insulating material with diameters of 0.1 to several microns and a density of up to 120000 pores cm⁻². We have used these micropore arrays for the detection of aqueous chlorine (Davis *et al* 1997). The arrays may be used as substrates for further electropolymerisation reactions, generating arrays of conducting polyaniline protrusions, consisting of just the polymer or alternatively containing entrapped

biological species (Barton *et al* 2004). Previous work within our group has utilised these microarrays containing entrapped enzymes for the amperometric detection of glucose (Barton *et al* 2004, Myler *et al* 2004), alcohol (Myler *et al* 2005). and a range of organophosphate pesticides (Pritchard *et al* 2004, Law *et al* 2005) with extreme sensitivity (10^{-17} M).

One difficulty often encountered when using sensors for practical analytical applications is that the species being detected can in some situations be present only at very low concentration while being contained within a complex biological system such as blood. This means that any sensor must display high sensitivities and also low non-specific adsorption of possible foulants or interferents. As can be seen from previous work using enzymes, use of microelectrodes rather than planar electrodes can lead to extremely high sensitivities (Pritchard *et al* 2004, Law *et al* 2005). Attempts therefore were made within this study to determine whether the use of microelectrodes rather than planar electrodes within immunosensors similar to those previously reported (Grant *et al* 2003, 2005) would lead to sensitivity enhancements. Microelectrode arrays containing entrapped anti-BSA were constructed and their performance compared with our previous work on planar, entrapped sensors.

A disadvantage associated with the entrapment method used within much of our previous work for antibody immobilisation is that the antigen will often be too bulky to diffuse through the polymer matrix and so only antibodies located at the surface of the polymer film or microelectrode - and suitably orientated, will be available for antigen binding. Other work comparing monolayers of randomly and specifically orientated antibody fragments (Bonroy *et al* 2006) showed that immunosensor responses typically double when the fragment is specifically orientated.

Digoxin (supplementary information, figure S2) is a cardiac drug, widely used in the treatment of various heart conditions such as atrial fibrillation and atrial flutter, with a narrow therapeutic range of 0.8-2.0 ng ml⁻¹ (Terra *et al* 1999). Previous work by our group demonstrated the construction of an immunosensor for digoxin, however, these sensors were only capable of detecting the antigen in the mg-μg ml⁻¹ ranges (Grant *et al* 2003). The anti-digoxin antibodies used in this early study were entrapped within a planar, electropolymerised film. We therefore within this work also compare results obtained using an affinity method to graft antibodies to the surface of the film with those obtained previously by entrapment (Grant *et al* 2003) in an attempt to improve sensitivity.

The focus of this paper is not just to describe the development of particular sensors - but rather to compare the behaviour of sensors fabricated using a variety of methods, namely our earlier work on entrapment in planar polymer films with affinity grafted planar films and also entrapment of the antibodies within conductive polymer protrusions. As will be demonstrated, both methods lead to an enhancement in sensitivity.

2. Experimental

2.1. Materials and equipment

Sodium dihydrogen orthophosphate, disodium hydrogen orthophosphate, sodium chloride and hydrochloric acid were obtained from BDH (Poole, Dorset, UK). Aniline, polyclonal human anti-IgG (AIgG), biotin 3-sulfo-N-hydroxysuccinimide, the biotinylation kit (part no. BK101), neutravidin, human serum albumin (HSA), bovine serum albumin (BSA), anti-bovine serum albumin (ABSA, developed in rabbit), digoxin, anti-digoxin (developed in rabbit-whole antiserum), sodium acetate,

acetic acid, sodium perchlorate, potassium ferrocyanide and potassium ferricyanide were obtained from Sigma-Aldrich, Gillingham, Dorset, UK. All water used was obtained from a Purelab UHQ Deioniser (Elga, High Wycombe, UK). Commercial screen-printed carbon electrodes (Figure S1, supplementary information) containing carbon working and counter electrodes and an Ag/AgCl reference electrode were obtained from Microarray Ltd, Manchester, UK. The surface area of the working electrode was 0.2178 cm^2 . AC impedance measurements were performed using an ACM Auto AC DSP frequency response analyser (ACM Instruments, Grange-over-Sands, UK). Cyclic voltammetry was performed using a Sycopel potentiometer (Sycopel Scientific, Tyne & Wear, UK) to electrodeposit polyaniline.

Aniline buffer (pH 1-2) was prepared containing 0.5 mol l^{-1} KCl, 0.3 mol l^{-1} HCl and 0.2 mol l^{-1} aniline. Phosphate buffer (PBS, pH 7.4) was prepared comprising 52.8 mmol l^{-1} disodium hydrogen orthophosphate 12-hydrate, 13 mmol l^{-1} sodium dihydrogen orthophosphate 1-hydrate and 5.1 mmol l^{-1} sodium chloride. Acetate buffer (pH 4.0) was prepared comprising 0.4 mol l^{-1} sodium acetate, 0.4 mol l^{-1} acetic acid and 0.4 mol l^{-1} sodium perchlorate.

The anti-digoxin was supplied as a solution in whole antiserum and was purified using a 5 ml protein G-column (Pharmacia). IgG fraction was eluted using glycine buffer (pH 2.7) and dialyzed overnight. For antibody biotinylation, the procedure outlined in the BK101 kit was followed (see manufacturers instructions for details). The biotinylated anti-digoxin was very dilute (0.01 mg ml^{-1}) and was concentrated using a Centriprep centrifugal filter unit (Millipore, Hertfordshire, UK) fitted with an Ultracel YM-30 membrane containing glycerol, to prevent drying. This procedure also ensured the removal of sodium azide from the antibody solution. The procedure involved three subsequent centrifugations in a cold room (4°C), each for 20

minutes at 30,000 rpm; the final concentration was 0.5 mg ml⁻¹. Biotinylated antibodies were kept frozen in aliquots of 200 µl until required.

2.2. Formation of microarrays.

Sonochemically fabricated microarrays were constructed as previously described (Barton *et al* 2004). To deposit the insulating layer, a 5 mmol l⁻¹ solution of 1,2-diaminobenzene in pH 7.4 phosphate buffer was utilised. Prior to the immersion of the carbon electrode, the monomer solution used was thoroughly purged with N₂ for 20 minutes in a sealed cell to provide an oxygen free atmosphere. An initial 1-second blast of ultrasound was also applied to a submerged electrode to displace air bubbles trapped at the surface of the electrodes. Homogenous insulation of a planar carbon electrode was achieved by sequentially scanning the working electrode potential from 0 mV through to +1000 mV (vs. Ag/AgCl) and back to the starting potential at a scan rate of 50 mVs⁻¹ for 20 sweeps.

Sonication experiments were performed using a custom built 2 kW, 25 kHz ultrasound tank with internal dimensions of 750 x 750 x 600 mm (working volume 750 x 750 x 500 mm) (Ultrawave Ltd., Cardiff, UK). Ultrasound was applied at a frequency of 25 KHz for 10 seconds duration.

2.3. Incorporation of antibody within microarrays via electrochemical deposition.

A 0.2 M aniline hydrochloride solution was prepared in a pH 4.0 acetate buffer. The solution pH fell to approximately 2.6 upon addition of monomer. Monoclonal antibody receptor was incorporated into the buffered monomer solution prior to polymerisation at a resultant concentration of 0.5 mg ml⁻¹. The pH of the monomer solution increases upon addition of antibody, this was monitored to ensure

the pH remained below 4.0 so that the conductive protonated ‘emeraldine’ form of polyaniline was deposited at the working electrode. Electrochemical deposition of the polyaniline was performed by sequentially cycling the working electrode potential from -200 mV through to $+800$ mV (vs. Ag/AgCl) and back to the starting potential at a scan rate of 50 mVs⁻¹. A linear sweep from -200 to $+800$ mV (50 mVs⁻¹) was performed at the end of cyclic voltammetry to leave the polyaniline in its protonated emeraldine salt form. This led to formation of polyaniline protrusions containing entrapped antibodies as previously described (Barton *et al* 2004, Law *et al* 2005).

2.4. Construction of planar antibody electrodes via an affinity protocol

Anti-digoxin was immobilised at the surface of planar electrodes by the methods previously described (Garifallou *et al* 2007, Tsekenis *et al* 2008) and the immunosensor structure is shown schematically in figure 2. The potentiodynamic electrodeposition of polyaniline from aniline buffer, pH 1-2 into the microelectrode array was achieved electrochemically as described for the microarrays.

30 μ l of biotin-sulfo-NHS (10 mg ml⁻¹ in water) was placed on the working electrode surface for 24 hours. The sensors were rinsed with copious water and 30 μ l of neutravidin (10 μ g ml⁻¹ in water) placed on the working electrode for 1 hour - followed by further rinsing in water. 30 μ l biotinylated anti-digoxin (0.5 mg ml⁻¹ in water, 1 hour) was then added followed by rinsing. Finally, non-specific interactions were blocked by HSA (10^{-6} mol l⁻¹ in PBS, 1 hour).

2.5. Determination of antigen concentration

AC impedance measurements were performed using an ACM Auto AC DSP frequency response analyser. Following immobilisation of antibody, impedance

analyses were performed from 1 Hz to 10,000 Hz (\pm 5 mV amplitude perturbation) in pH 7.4 phosphate buffer, i.e. containing no antigen, as a baseline trace. This buffer solution did, however, contain a 50:50 mixture of $[\text{Fe}(\text{CN})_6]^{3-/4-}$, at a concentration of 10 mmol l^{-1} as redox mediator so as to perform faradaic impedance spectroscopy. The potential of the electrochemical cell is offset to the formal potential of the redox probe ($+0.12 \text{ V vs. Ag/AgCl}$ identified via amperometric cyclic voltammetry). Following the recording of a baseline spectral trace (0 ng ml^{-1} antigen), the same sensor is used for all concentrations and exposed for 30 minute time periods to the increasing concentrations of antigen in phosphate buffered test solution.

After each 30 minutes exposure to a known concentration, the sensor was thoroughly flushed with 50ml of pH 7.4 phosphate buffer (containing $[\text{KFe}(\text{CN})_6]^{3-/4-}$ & no antigen) to remove any non-specifically adsorbed matter before ac impedance spectra were recorded in the phosphate buffered test solution (containing $[\text{KFe}(\text{CN})_6]^{3-/4-}$ & no antigen). This sensor was then exposed to an increasing antigen concentration and the process repeated for the full range of applied antigen concentrations under investigation. Traces recorded may then be compared to the baseline trace. Immunosensors were also tested where the electrode was exposed to a diminishing series of antigen concentrations i.e. starting with the highest and gave similar results (Garifallou 2008).

The electrode assemblies were found to be very stable, for example a sensor placed in pH 7.4 phosphate buffer (containing $[\text{KFe}(\text{CN})_6]^{3-/4-}$ showed no change in the ac impedance curves even after 90 minutes equilibration (Tsekenis 2008).

3. Results and discussion

3.1. Impedance results for planar, affinity immobilised anti-digoxin electrodes:

Figure 3 shows the (a) Bode and (b) Nyquist curves obtained for a planar polyaniline/anti-digoxin modified, carbon electrode exposed to various concentrations in the range of 0-10 ng ml⁻¹ of antigen. The Nyquist curve (figure 3b) demonstrates that the Z' (real) component of the impedance increases steadily with decreasing frequency whereas the Z'' (imaginary) component increases to a maximum value (at frequencies in the range 5-10 Hz) before falling as the frequency approaches 1 Hz. This type of impedance spectrum is indicative of a surface-modified electrode system where the electron transfer is slow and the impedance is controlled by the interfacial electron transfer (Katz and Willner 2003).

As can be seen, there is a steady decrease in impedance as antigen concentration increases towards a concentration of about 1.5 ng ml⁻¹. Levels of 2 ng ml⁻¹ and 10 ng ml⁻¹ did not lead to even lower impedances, but rather tend towards a plateau, indicating saturation of the specific binding sites. Any further changes in impedance beyond 1.5 ng ml⁻¹ are likely to be due to non-specific interactions. The corresponding Bode plots (figure 3a) also show a decrease in the total impedance as the digoxin levels increase. This indicates that the binding of digoxin is facilitating electron transfer between the electrode and the redox probe. Since the therapeutic range is 0.8-2.0 ng ml⁻¹ (Terra *et al* 1999) this indicates that these sensors will be sufficiently sensitive and in fact there may be a need to undertake some dilution of the sample. However the range of these sensors is unfortunately rather small, which may preclude their use in real situations. What is of interest though is the much higher sensitivity compared to digoxin sensors fabricated by entrapment, indicating that controlled immobilisation does lead to enhanced sensitivity.

The impedance spectra consists of two components, the real (Z') component where the impedance in phase with the AC potential waveform is measured and the

imaginary (Z'') where the impedance is 180° out of phase. Previous work by our group has demonstrated that in these type of systems, the increase in the real component dominated the total increase in the impedance and perhaps more importantly the real component offers far greater reproducibility in comparison to the imaginary contribution (Garifallou *et al* 2007, Tsekenis *et al* 2008).

Our previous work demonstrated that the sensors of this type gave the largest relative changes at the lower frequencies (Garifallou *et al* 2007, Tsekenis *et al* 2008). Calibration curves could be drawn (figure 4a) showing the percentage decrease in Z' at 1 Hz across a range of antigen concentrations. Again these show a relationship between antigen concentration and the decrease in Z' .

Non-specific interactions have the potential to either exaggerate or mask specific interactions. Whereas specific binding of antigens will only occur when their antibodies is present, electrodes fabricated using a non-specific antibody should undergo the same non-specific binding events as those fabricated using specific antibodies. The calibration curve showing the percentage decrease in Z' at 1 Hz is shown for sensors fabricated using an identical protocol except that the specific antibody is replaced by a non-specific IgG antibody (figure 4b). As can clearly be seen, there is a much lower response for the non-specific antibody, showing that although there are non-specific interactions, between the concentration ranges of 0-2 ng ml^{-1} , they comprise a minor component of the detected response.

Once the non-specific responses have been subtracted (figure 4a - figure 4b), a corrected plot (figure 4c) shows the calibration curve for the corrected sensor response. Between a concentration range of 0-1.5 ng ml^{-1} , there is a clear correlation of the corrected impedance change with the concentration. The limit of detection, calculated as 3x the standard deviation of the baseline sample of this system

(Analytical methods committee, 1987) is approximately 0.1 ng ml^{-1} . Our previous system using entrapment of digoxin within a polymer film combined with pulsed waveform detection (Grant *et al* 2003) was only capable of resolving digoxin at levels higher than $50 \text{ } \mu\text{g ml}^{-1}$, so as can be seen the combination of an ac interrogation protocol and an affinity based immobilisation procedure leads to at least a two orders of magnitude increase in sensitivity. The responses for 10 ng ml^{-1} digoxin (not shown in plots) were indistinguishable from those at 2 ng ml^{-1} .

3.2. Impedance results for entrapment immobilised anti-BSA microelectrodes:

Impedance traces for polyaniline microelectrode sensors containing entrapped ABSA were obtained as for the anti-digoxin based electrodes. These were very similar in appearance to those obtained for previous electrodes, again indicating a electrochemical system where the electron transfer is slow and the impedance is controlled by the interfacial electron transfer (Katz and Willner 2003). Rather than just studying the change in Z' at 1 Hz, it was decided to undergo a more detailed investigation of the electrochemical system. A computer fitting of the experimental data to a theoretical model, represented by a simple equivalent circuit, may be performed by the software accompanying the frequency response analyser. In this case, the interface is modelled by an equivalent circuit (supplementary information, figure S3), also called a Randles circuit (Randles, 1947), consisting of a double-layer capacitor in parallel with a polarization resistor (also known as a charge transfer resistor with certain constraints) and a Warburg impedance, connected in series with a resistor that measures the resistance of the electrolyte solution. For a more thorough evaluation of the data obtained, the changes in the Nyquist curves may be translated into electron transfer resistance changes to provide a clear and consistent format.

The relative electron transfer resistance changes from the baseline response at each concentration of BSA for a typical electrode modified with ABSA are plotted in figure 5a. The electron transfer resistance increases with increasing BSA concentration and demonstrates that an entrapped ABSA immunosensor gave a linear response to the analyte from 0 ng ml⁻¹ to 100 ng ml⁻¹ ABSA.

The insulation of the modified electrode upon formation of stable antibody-antigen immunocomplexes hinders the electron transfer kinetics of the redox probe resulting in the increase of electron transfer resistance. The electron transfer resistance increases with increasing antigen concentration for both types of electrode. The limit of detection (three times the standard deviation of the baseline value) of the entrapped ABSA immunosensor is 1 ng ml⁻¹. There is negligible change from 100 ng ml⁻¹ to 300 ng ml⁻¹ suggesting that the immunosensor approaches saturation.

Non-specific interactions have the potential to interfere with immunosensor performance, leading to erroneously elevated results. For this reason, identical sets of immunosensors were fabricated by both methods utilising a non-specific IgG antibody in place of the specific ABSA antibody. Results for these electrodes were obtained in exactly the same manner as for the specific electrodes. From the Nyquist plots for these systems (not shown), it could be seen that while binding of BSA to the non-specific immunosensors occurs, the responses are smaller than for ABSA modified sensors. A calibration plot for this system can also be drawn (figure 5b) and shows a linear-type non-specific response is observed for the affinity based anti-IgG immunosensor from 1 to 100 ng ml⁻¹ BSA with a plateau above this concentration. Upon comparison of figure 5a with figure 5b, it is apparent that approximately 50% of the ABSA-affinity immobilised sensor response encountered is, in fact, non-specific.

This is most likely due to the fact that BSA is a protein with a high affinity for surfaces and no blocking reagents have been utilised for these electrodes.

To obtain a calibration profile, in terms of 'corrected' electron transfer resistance change for an ABSA immunosensor, accounting for any non-specific responses, the non-specific response was subtracted from the specific response over the entire analytical concentration range. In total 10 ABSA immobilised sensors of each type and 10 corresponding anti-IgG immobilised sensors were interrogated over their active concentration range, to allow an assessment of the reproducibility of the responses for this system. Results are presented in figure 6. The error bars are the standard deviations obtained for the 10 matched sensor pairs from the mean 'corrected' values.

From figure 6 a linear response was observed for the immunosensors from 0-100 ng ml⁻¹ BSA. Figure 6 (inset) shows an expanded view from 0 to 10 ng ml⁻¹ BSA and shows linear behaviour with R²>0.99. At concentrations above 100 ng ml⁻¹, the sensor becomes saturated. From the standard deviations obtained, we can say that discrimination of BSA antigen analyte is possible at 5 ng ml⁻¹. The limit of detection of the ABSA immunosensor is 1.5 ng ml⁻¹ BSA and is calculated from 3x the standard deviation of the baseline response and extrapolated from the line of best-fit according to IUPAC guidelines (Analytical methods committee, 1987). Previous work (Grant *et al* 2003, 2005) allowed detection of BSA at levels as low as 10 µg ml⁻¹. As can be seen the use of polyaniline microelectrodes has greatly increased sensitivity, although in this instance there is a problem with high non-specific responses.

3.3 Stability of the BSA immunosensors and regeneration studies.

Although a long-term sensor stability test was not performed, a batch of 18 sensor pairs was assessed from storage in dry state, at 4°C, for a period of 12 weeks. Again an identical experimental protocol was employed for electrochemical impedance interrogation and the ‘corrected’ electron transfer change was the analysis method for response recovery.

Every 2 weeks a set of 3 matched sensor pairings was removed from storage and interrogated over the full BSA antigen analyte concentration range from 1 to 300 ng ml⁻¹. After 2 weeks no loss of sensor response occurred but after 4 weeks there was a 10% loss in response and further steady decreases until after 10 weeks storage only 10% of the original response was detected.

Some of our previous work demonstrated that acid washing of some immunosensors led to their regeneration (Barton 2007). Attempts were made to see whether it was possible to regenerate the sensors by acid washing. 5 ABSA-immobilised sensors and 5 matched non-specific AIgG-immobilised sensors are exposed to the full interrogation procedure prior to reversibility investigations. In order to split the antibody-antigen complex and to regenerate the sensors, 0.1M HCl acidic buffer (pH 2.3) was applied for 3 separate 1 minute time periods. In between each acidic buffer exposure, pH 7.4 PBS was used to rinse the sensor surface. Finally the sensors were rinsed with 50ml PBS to produce PSA-free sensors which could then be used for fresh analysis. Unfortunately in all cases the washing removed all activity. An identical baseline response could be achieved which suggests that the sensor surface integrity remains, yet the antigen recognition and binding capabilities of the receptor antibodies are severely damaged by the treatments.

4. Conclusions

Our work verifies several fabrication techniques and an ac experimental interrogation protocol as a viable approach towards the labelless sensing of BSA and digoxin. Affinity based sensors where anti-digoxin is immobilised on planar electrodes using avidin-biotin interactions have been shown to display much higher sensitivities (by two orders of magnitude, capable of detection of ng ml^{-1} levels of antigen) than sensors developed in earlier work utilising entrapment within planar conductive polymer electrodes as the method of immobilisation. Low non-specific binding of these electrodes was also observed. However the range of these electrodes was very limited which could preclude their use in real analyses.

Similarly sensors developed where ABSA is entrapped in conductive polymer microelectrodes rather than planar polymer films have been studied. The microelectrode array sensors were three orders of magnitude more sensitive, again allowing detection of ng ml^{-1} levels of antigen. These types of sensors however displayed higher non-specific binding. However BSA is a protein noted for its high binding ability to surfaces and future sensors for other analytes will include a BSA blocking step to reduce non-specific interactions.

The next step involved combining these two methods in an attempt to enhance the sensitivity levels even further. Sensors have been developed involving a multi-step procedure. Initially conductive polyaniline microarrays were constructed. The polyaniline was then modified with biotinylation reagents and biotinylated antibodies immobilised by the affinity procedures described above. Finally the sensors are blocked with HSA. Ongoing work has demonstrated the construction of sensors for prostate specific antigen, neuron specific enolase and the stroke marker protein S-100[β]. *These immunosensors have been shown capable of quantifying antigens at levels as low as 1 pg ml^{-1} , these will be the subject of a further series of*

publications to be submitted for publication shortly and will be described in detail at the 10th World Congress in Biosensors, Shanghai, May 14th-18th 2008.

Acknowledgements

This work, including funding for ACB, G-Z G, GT and FD, has been supported by the European Community QLRT-2001-02583 (SMILE) and NMP2-CT-2003-505485, (ELISHA) Framework VI contracts.

References

Analytical Methods Committee, 1987. *Analyst* 112, 199-204.

Barnett, D., Laing, D. G., Skopec, S., Sadik, O. A., Wallace, G. G., 1994. *Anal. Lett.* 27, 2417-2429.

Barton, A.C., Collyer, S. D., Davis, F., Gornall, D. D., Law, K. A., Lawrence, E. C. D., Mills, D. W., Myler, S., Pritchard, J. A., Thompson, M., Higson, S. P. J., 2004. *Biosens. Bioelec.* 20, 328-337.

Barton, A.C., 2007, PhD Thesis, Cranfield University.

Bender, S. Sadik, O. A., 1998. *Environ. Sci. Tech.* 32, 788-797.

Bonroy, K., Frederix, F., Reekmans, G., Dewolf, E., De Palma, R., Borghs, G., Declerck, P., Goddeeris, B., 2006. *J. Immunolog. Met.* 312, 167-181.

Clark, L. C., Lyons, I. R., 1962. *Ann New York Academy Sci.* 102, 29-45.

Cosnier S., 2005. *Electroanalysis* 17, 1701-1715.

Davis, F., Collyer, S. D., Gornall, D. D., Law, K. A., Mills, D. W., Higson, S. P. J., 2007. *Chimica Oggi/Chemistry Today* 25, 28-31.

Diaz-Gonzalez, M., Gonzalez-Garcia, M. B., Costa-Garci, A., 2005. *Electroanalysis* 17, 1901-1918.

Garifallou, G.-Z., Tsekenis, G., Davis, F., Higson, S. P. J., Millner, P. A., Pinacho, D. G., Sanchez-Baeza, F., Marco, M.-P., Gibson, T. D. 2007. *Anal. Lett.* 40, 1412-1442.

Garifallou, G.-Z., 2008, PhD Thesis, Cranfield University.

Grant, S., Davis, F., Pritchard, J. A., Law, K. A., Higson, S. P. J., Gibson, T. D., 2003. *Anal. Chim. Acta.* 495, 21-32.

Grant, S., Davis, F., Law, K. A., Barton, A. C., Collyer, S. D., Higson, S. P. J., Gibson, T. D., 2005. *Anal. Chim. Acta.* 537, 163-168.

Higson, S. P. J., 'Sensor', International Patent: PCT/GB96/0092, 1996.

John, R., Spencer, M., Wallace, G. G., Smyth, M. R., 1999. *Anal. Chim. Acta.* 249, 381-385.

- Katz, E, Willner, I., 2003. *Electroanalysis* 15, 913-947.
- Law, K. A., Higson, S. P. J., 2005. *Biosens. Bioelec.* 21, 1914-1924.
- Myler, S., Eaton, S., Higson, S. P. J., 1997. *Anal. Chim. Acta.* 357, 55-61.
- Myler, S., Davis, F., Collyer, S. D., Higson, S. P. J., 2004. *Biosens. Bioelec.*, 20, 408-412.
- Myler, S., Davis, F., Collyer, S. D., Gornall, D. D., Higson, S. P. J., 2005. *Biosens. Bioelec.* 21, 666-671.
- Pritchard, J. A., Law, K. A., Vakurov, A., Millner, P. A., Higson, S. P. J., 2004. *Biosens. Bioelec.* 20, 765-772.
- Randles, J.E.B. 1947, *Discussions of the Faraday Society*, 1, .11-19.
- Rodriguez-Mozaz, S., de Alda, M. J. L., Barcelo, D., 2006. *Anal. Bioanal. Chem.* 386, 1025-1041.
- Sadik, O. A., John, M. J., Wallace, G. G., Barnett, D., Clarke, C., Laing, D. G., 1994. *Analyst* 119, 1997-2000.
- Terra, S. G., Washam, J. B., Dunham, G. D., Gattis, W. A., 1999. *Pharmacotherapy* 19(10) 1123-1126.

Tsekenis, G., Garifallou, G. Z., Davis, F., Millner, P. A., Gibson, T. D., Higson, S. P.

J.2008. *Anal. Chem.*, 20, 2058-2062.

Tsekenis, G., 2008, PhD Thesis, Cranfield University.

Yalow, R. S., Berson, S. A., 1959. *Nature*. 184, 1648-1649.

LIST OF FIGURES.

Figure 1. Formation of polyaniline microarrays (a) deposition of insulating layer (b) sonochemical formation of pores (c) polymerisation of aniline.

Figure 2. Schematic of the affinity binding procedure used to immobilise anti-digoxin

Figure 3. (a) Bode and (b) Nyquist plots of a typical specific anti-digoxin modified electrode exposed to various concentrations in the range 0-10.0 ng ml⁻¹ of digoxin in PBS.

Figure 4. Calibration curves showing the increase in the real component of impedance (in the range 0-2.0 ng ml⁻¹ digoxin) at 1Hz for: (a) specific anti-digoxin modified electrodes exposed to varying concentrations of antigen (b) IgG modified electrodes exposed to antigen under identical conditions (c) corrected calibration curves where the non-specific response has been subtracted from the specific response (curve a – curve b). All data points are means for the responses of three electrodes; error bars give a measure of the reproducibility of the system.

Figure 5. Calibration plot showing changes in electron transfer resistance vs. BSA concentration. (a) entrapped ABSA (0-300 ng ml⁻¹) (b) entrapped anti-IgG (0-300 ng ml⁻¹)

Figure 6. Corrected calibration curves where the non specific response has been subtracted from the specific response (0-300 ng ml⁻¹) (inset) corrected calibration plot (0-10 ng ml⁻¹).

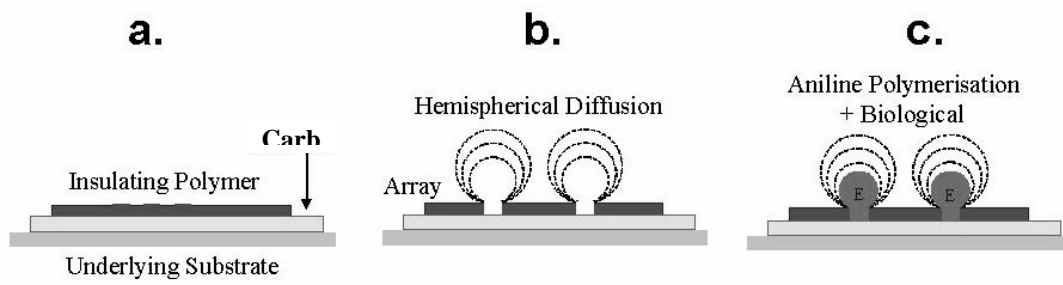


Fig 1

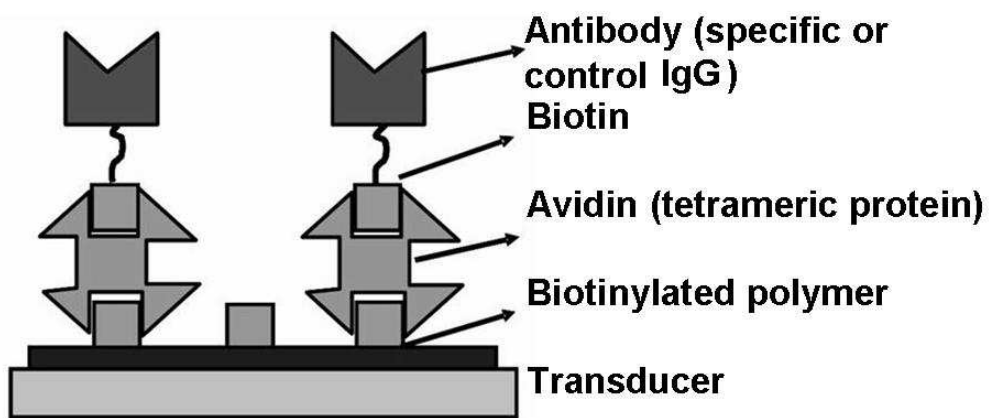


Fig 2

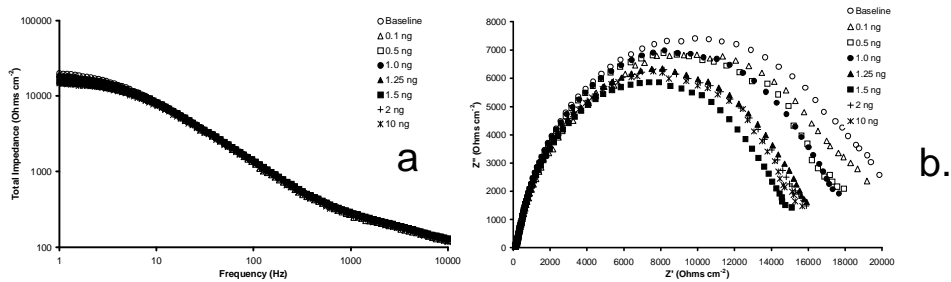


Fig 3

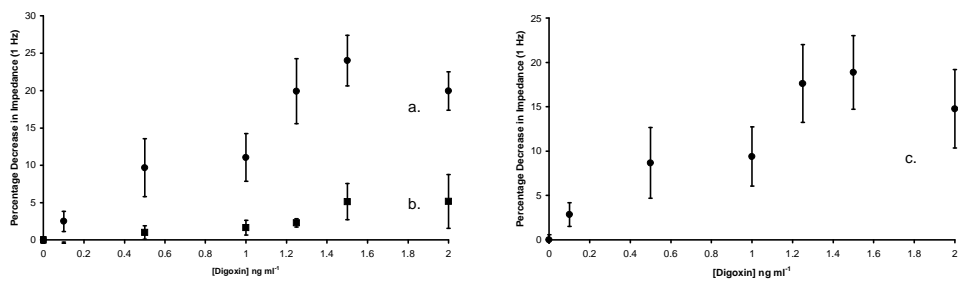


Fig 4

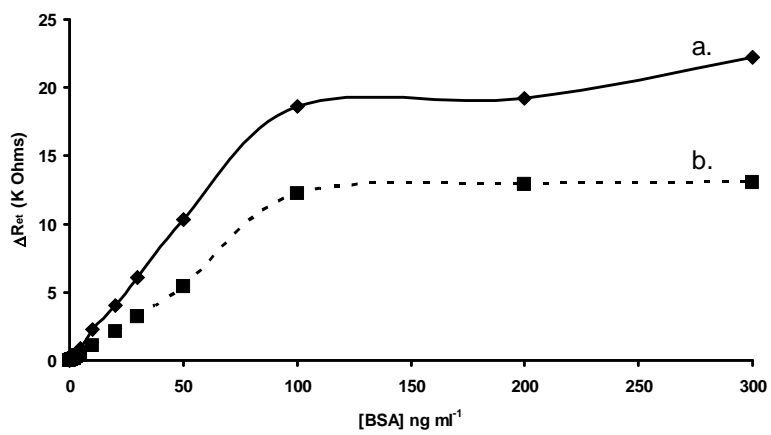


Fig 5

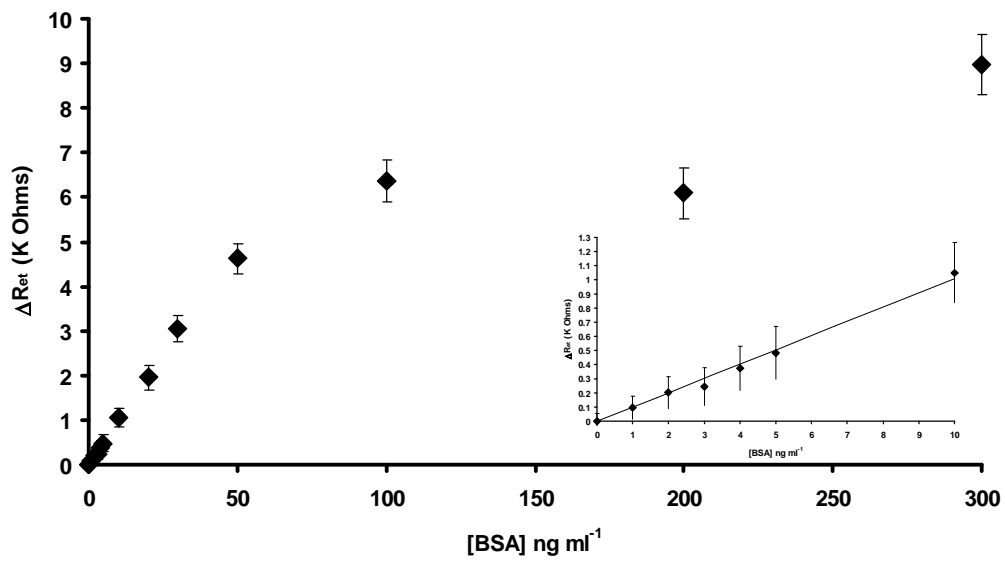


Fig 6

Labelless AC Impedimetric Antibody Based Sensors with pg ml^{-1} Sensitivities for Point-Of-Care Biomedical Applications.

Andrew C. Barton¹, Goulielmos-Zois Garifallou¹, Frank Davis¹, Stuart D. Collyer², Georgios Tsekenis¹, Paul A. Millner³, Tim D. Gibson⁴ and Séamus P. J. Higson^{*1}.

Supplementary Information

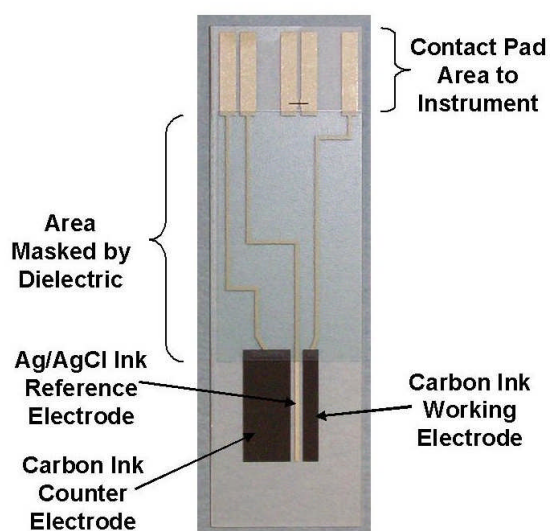


Figure S1. Screen-printed carbon electrodes used within this work.

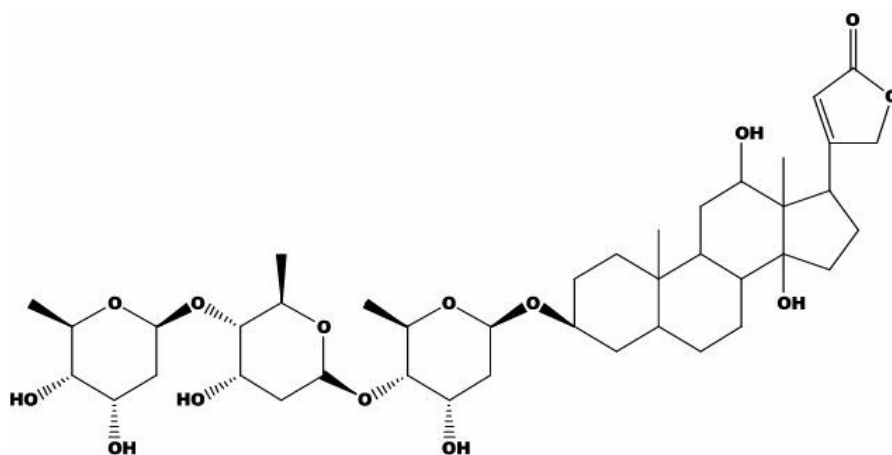


Figure S2. Structure of digoxin.

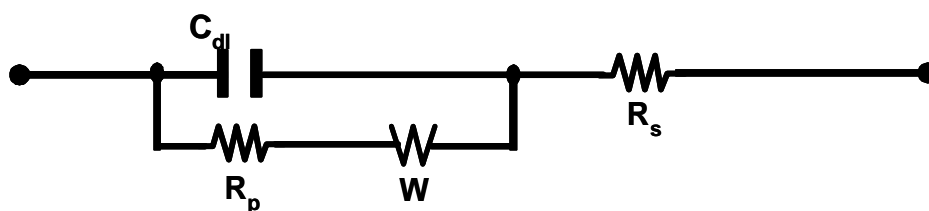


Figure S3. An equivalent circuit representing each component at the interface and in the solution during an electrochemical reaction is shown for comparison with the physical components. C_{dl} , double layer capacitor; R_p , polarization resistor; W , Warburg resistor; R_s , solution resistor.